TU Delft

Delft University of Technology

Characteristic fracture spacing in primary and secondary recovery for naturally fractured reservoirs

Gong, J.; Rossen, W. R.

DOI
10.1016/j.fuel.2018.02.046

Publication date
2018

Document Version
Final published version

Published in
Fuel: the science and technology of fuel and energy

Citation (APA)
Gong, J., & Rossen, W. R. (2018). Characteristic fracture spacing in primary and secondary recovery for naturally fractured reservoirs. *Fuel: the science and technology of fuel and energy*, *223*, 470-485. https://doi.org/10.1016/j.fuel.2018.02.046

Important note
To cite this publication, please use the final published version (if applicable).
Please check the document version above.

Copyright
Other than for strictly personal use, it is not permitted to download, forward or distribute the text or part of it, without the consent of the author(s) and/or copyright holder(s), unless the work is under an open content license such as Creative Commons.

Takedown policy
Please contact us and provide details if you believe this document breaches copyrights.
We will remove access to the work immediately and investigate your claim.

This work is downloaded from Delft University of Technology.
For technical reasons the number of authors shown on this cover page is limited to a maximum of 10.

Fuel 223 (2018) 470–485

Contents lists available at ScienceDirect

Fuel

journal homepage: www.elsevier.com/locate/fuel

Full Length Article

Characteristic fracture spacing in primary and secondary recovery for naturally fractured reservoirs

J. Gong*, W.R. Rossen

Department of Geoscience & Engineering, Delft University of Technology, Delft 2628 CN, The Netherlands

ARTICLE INFO

Keywords:
Fractured reservoir
Fracture spacing
Dual-porosity
Dual-permeability
Peclet number
Oil recovery

ABSTRACT

If the aperture distribution is broad enough in a naturally fractured reservoir, even one where the fracture network is highly inter-connected, most fractures can be eliminated without significantly affecting the flow through the fracture network. During a waterflood or enhanced-oil-recovery (EOR) process, the production of oil depends on the supply of injected water or EOR agent. This suggests that the characteristic fracture spacing (or shape factor) for the dual-porosity/dual-permeability simulation of waterflood or EOR in a naturally fractured reservoir should account not for all fractures but only the relatively small number of fractures carrying almost all the injected water or EOR agent ("primary," as opposed to "secondary," fractures). In contrast, in primary production even a relatively small fracture represents an effective path for oil to flow to a production well. This distinction suggests that the "shape factor" in dual-permeability reservoir simulations and the repeating unit in homogenization should depend on the process involved: specifically, it should be different for primary and secondary or tertiary recovery. We test this hypothesis in a simple representation of a fractured region with a non-uniform distribution of fracture flow conductivities. We compare oil production, flow patterns in the matrix, and the pattern of oil recovery with and without the "secondary" fractures that carry only a small portion of injected fluid.

The role of secondary fractures depends on a dimensionless ratio of characteristic times for matrix and fracture flow (Peclet number), and the ratio of flow carried by the different fractures. In primary production, for a large Peclet number, treating all the fractures equally is a better approximation of the original model, than excluding the secondary fractures; the shape factor should reflect both the primary and the secondary fractures. For a sufficiently small Peclet number, it is more accurate to exclude the secondary fractures in calculation of the shape factor in the dual-porosity/dual-permeability models than to include them and, in effect, assume they play an equally important role in transport to and from the matrix. For waterflood or EOR, in most cases examined, the appropriate shape factor or the repeating-unit size should reflect both the primary and secondary fractures. If the secondary fractures are much narrower than the primary fractures, then it is more accurate to exclude them for calculating the shape factor in a dual-porosity/dual-permeability model. Yet-narrower "tertiary fractures" are not always helpful for oil production, even if they are more permeable than matrix. They can behave as capillary barriers to imbibition, reduce oil recovery.

We present a new definition of Peclet number for primary and secondary production in fractured reservoirs that provides a more accurate predictor of the dominant recovery mechanism in fractured reservoirs than the previously published definition.

1. Introduction

A significant amount of hydrocarbon reserves across the world resides in naturally fractured reservoirs [1]. Accurate simulation of oil recovery is required for the efficient exploitation of these naturally fractured reservoirs. However, because of the complexity and limited information regarding the sub-surface fracture networks, field-scale reservoir simulation requires simplified description of reservoir conditions.

If the fracture network is well-connected, this is often done with a dual-porosity or dual-permeability (DP/DK) simulation. In the DP/DK concept, the fracture and matrix systems are treated as separate domains; the interconnected fractures serve as fluid-flow paths between injection and production wells, while the matrix provides fluid storage

* Corresponding author.
E-mail addresses: j.gong@tudelft.nl (J. Gong), w.r.rossen@tudelft.nl (W.R. Rossen).

https://doi.org/10.1016/j.fuel.2018.02.046
Received 28 February 2017; Received in revised form 10 December 2017; Accepted 8 February 2018
0016-2361/ © 2018 The Authors. Published by Elsevier Ltd. This is an open access article under the CC BY-NC-ND license (http://creativecommons.org/licenses/BY-NC-ND/4.0/).

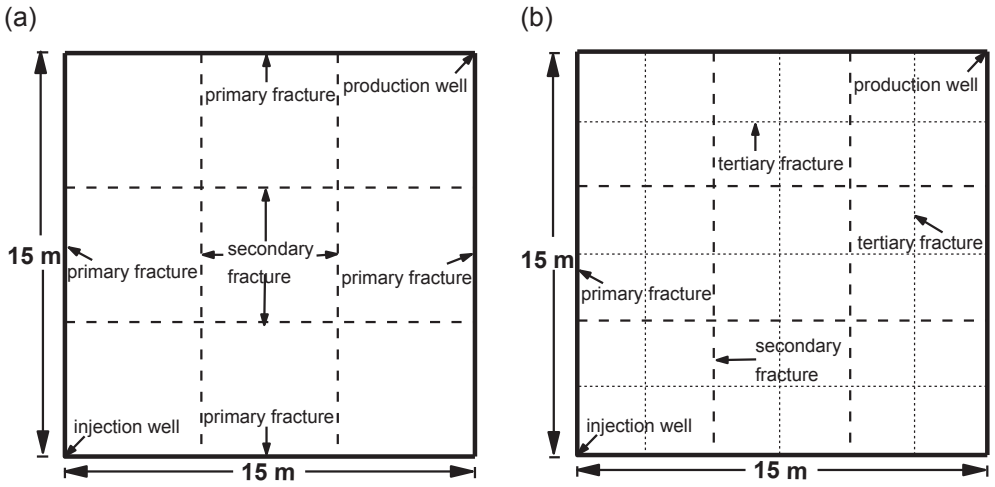

Fig. 1. Schematic of the region of study. The fractured region (unit cell) studied is 15 m × 15 m, with the injection and production wells placed at the bottom-left and the top-right corners, respectively. The injection well and production well are directly connected to the primary fractures without contacting the matrix block. (a) The region is bounded by the primary fractures, and penetrated by the secondary fractures. The number of the secondary fractures varies in different cases. In the case shown, $R_n = 1/3$. (b) Tertiary fractures are included in some cases. As in the cases examined below, there are as many tertiary fractures as primary and secondary fractures combined.

Table 1
Summary of petrophysical properties assumed in this study.

Parameter	Units	Value
Matrix porosity	fraction	0.2
Fracture porosity	fraction	1
Oil viscosity	Pa·s	0.0015
Water viscosity	Pa·s	0.00105
Oil density	kg/m^3	835
Water density	kg/m^3	999

for nearby fractures. Limited fluid flow between matrix blocks is allowed in dual-permeability models [2,3]. The interaction between the fracture network and matrix is represented by an exchange function which is characterized by a shape factor [4–6]. During the last few decades, discrete-fracture models (DFMs) have attracted increasing research interest. In these models, the fracture geometry and complex flow patterns in fracture networks are simulated more accurately [7–12]. However, DFMs are typically computationally too expensive for field-scale reservoir simulations. Also, even if detailed geological information is provided, it is difficult to predict the flow pattern through the fracture networks; some simplification is needed. Thus, although the DP/DK models are much-simplified characterizations of naturally fractured reservoirs, for the reservoirs with many fractures and a very high degree of interconnection, they are still more feasible than the DFM methods. To generate a DP/DK model, it is necessary to define average properties for each grid block, such as porosity, permeability and matrix-fracture interaction parameters (typical spacing or shape factor) [13]. Therefore, the discrete fracture network considered to generate the DP/DK model parameters is crucial. If homogenization is applied, the matrix-fracture exchange can be treated more accurately than in the DP/DK simulations [14], but, again, one needs a characteristic matrix-block size. However, if the fracture network shows non-uniform flow, then characterizing the fracture spacing or shape factor can be ambiguous.

As we presented in a previous study [15], even in a well-connected fracture network, there is a dominant sub-network which carries almost all the flow, but it is much sparser than the original network. In this study we refer to the fractures in the dominant sub-network as “primary” fractures, and the remaining fractures as “secondary” fractures. The primary fractures tend to be wider, but they are not necessarily the widest, longest or most highly connected fractures in the network [15]. The flow-path length of the dominant sub-network can be as little as 30% of that of the corresponding original fracture network. This suggests that in secondary production or enhanced oil recovery (EOR), the injected water or EOR agent flows mainly along a small portion of the fracture network. In contrast, in primary production even relatively small fractures can be an efficient path for oil to flow to a production well.

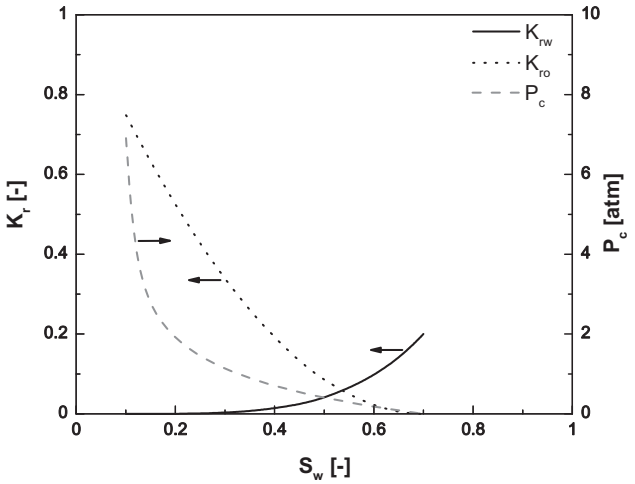

Fig. 2. The relative-permeability and capillary-pressure functions for the matrix blocks used in all the cases in this study.

In fractured reservoirs, oil is produced by different recovery mechanisms. During primary production, oil is mainly recovered by fluid expansion. In secondary production, spontaneous imbibition is the dominant recovery mechanism in water-wet reservoirs. In primary recovery, production depends only on a path to the well, whereas in secondary recovery or EOR, it depends on the injected agent reaching the matrix. This difference suggests that the relevant fracture spacing should be different for primary recovery and for waterflood or EOR [16].

The purpose of this study is to show the implications of non-uniform flow for the definition of the shape factor or characteristic fracture spacing in a dual-porosity/dual-permeability simulation of primary

Table 2
Values of parameters in Eqs. (1) and (2) adopted in this study.

Parameter	Units	Value
n_o	–	2
n_w	–	4
k_{ro}^o	–	0.75
k_{rw}^o	–	0.2
B	Pa	1.01×10^5

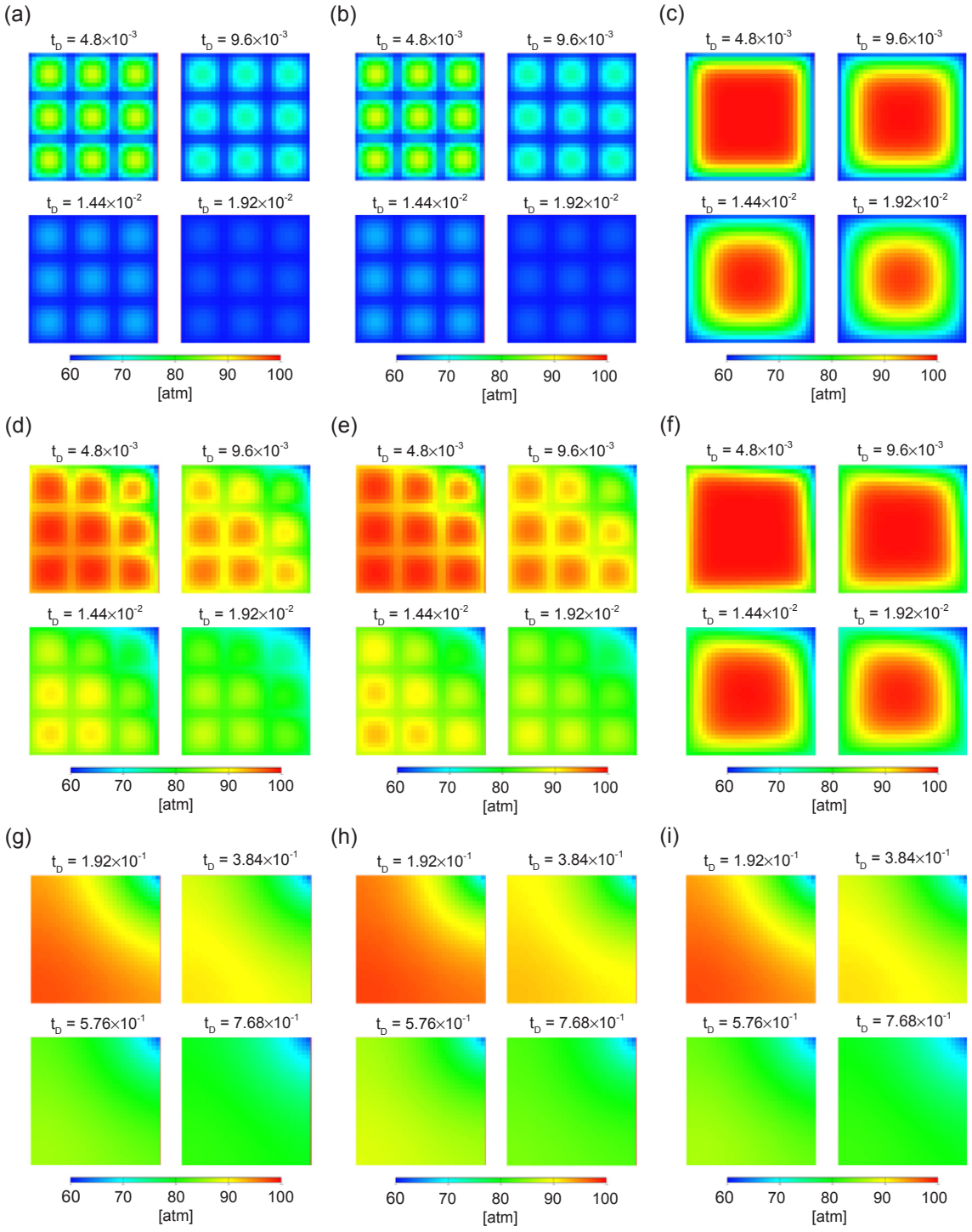

Fig. 3. Pressure distribution during primary production for different *Pe*, with R_d = 2.5 and R_n = 1/3. (a) *Pe* = 1,000, with all fractures; (b) *Pe* = 1,000, with all average fractures; (c) *Pe* = 1,000, without secondary fractures; (d) *Pe* = 10, with all fractures; (e) *Pe* = 10, with all average fractures; (f) *Pe* = 10, without secondary fractures; (g) *Pe* = 0.1, with all fractures; (h) *Pe* = 0.1, with all average fractures; (i) *Pe* = 0.1, without secondary fractures.

production and waterflood or EOR. To illustrate this point, we start with a simple fracture and matrix geometry. There are additional complications in the definition of shape factor when the matrix blocks are irregularly shaped and non-uniform in size [17–27]. As a start, we focus on the issue of non-uniform flow in the fractures, and choose a simple geometry to highlight this aspect.

2. Problem description

This study concerns the flow pattern within a fractured region (which can be seen as a unit cell in a DP/DK model) in primary production or a waterflood process. The roles that the primary and secondary or tertiary fractures play during primary and secondary recovery are studied. Within a unit cell, there is an interconnected network of the primary fractures. The unit cell defined by this network is inter-penetrated by the secondary fractures (the tertiary fractures are

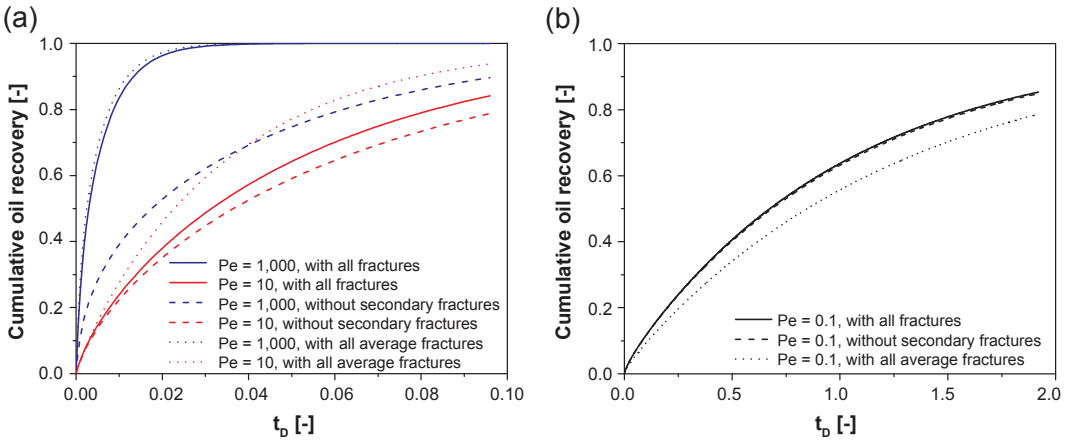

Fig. 4. Cumulative oil recovery during primary production for different *Pe*, with $R_d = 2.5$ and $R_n = 1/3$. The cumulative oil recovery is normalized by the producible oil for the given pressure reduction.

also included in some cases below). We examine a simplified representation of a unit cell. Specifically, we represent a region bounded by the primary fractures and penetrated by the secondary fractures (also by the tertiary fractures in some cases). A simulation grid block might contain many such unit cells. In our simple model, the primary fractures are wider, though in reality aperture is only one factor in determining which fractures carry most of the injected fluid [16].

The model employed here is illustrated in Fig. 1. It is a 2D, 15 m × 15 m region bounded by four primary fractures (with the same aperture) and penetrated by several secondary fractures. The tertiary fractures (narrower than the secondary fractures) are also included in some cases. To simulate flow through the primary fracture network on a larger scale, an injector and a producer are connected to the primary fractures and placed at the bottom left and top right corner, respectively. The matrix permeability (k_m) in both directions is the same, i.e. 0.5 md. The directional permeability (k_f) of the fractures along the fracture direction is given by $d^2/12$, where d is the fracture aperture, while the permeability in the direction perpendicular to the fracture is the same as the matrix permeability. The other petrophysical properties are listed in Table 1. The fracture cells are assigned zero capillary pressure and straight-line relative permeabilities. The matrix blocks are water-wet (Fig. 2). The relative-permeability and capillary-pressure functions for the matrix are [28–30]

$$k_{ro} = k_{ro}^{o}(1-S)^{n_o},\ k_{rw} = k_{rw}^{o}S^{n_w};\mathrm{S} \equiv \frac{S_w - S_{wr}}{1 - S_{wr} - S_{or}} \tag{1}$$

$$P_c(S) = -B\ln(S) \tag{2}$$

where S_w, S_{wr} and S_{or} are the water saturation, the irreducible water saturation and the residual oil saturation, respectively, n_o and n_w are the empirical parameters, k_{ro}^{o} and k_{rw}^{o} are the end-point oil and water relative permeabilities, respectively, and B is a constant. Their values are listed in Table 2.

3. Methodology

In order to identify the roles played by the primary and secondary or tertiary fractures, we examine the flow behavior in three cases: (1) all the fractures present; (2) the secondary or tertiary fractures are excluded; and (3) all the fractures present, but with the same aperture. Specifically, we give all the fractures the same aperture, which provides the same total conductivity for the fracture network as with the primary and secondary fractures in case (1). We call this case "all average fractures" in the results below. In case (3), all the fractures play a similar role, as is assumed in the traditional DP/DK concepts.

The results are analysed according to three dimensionless groups.

The Peclet number indicates the relative importance of advection and diffusion to the transport of a physical quantity in a given system. In this study, the intent is to represent the relative efficiency of matrix production and fracture flow: i.e., how conductive fractures are compared to matrix productivity. Details of our analysis can be found in the Appendix. Considering the different oil-recovery mechanisms in primary and secondary recovery (or EOR), we propose different Peclet numbers for the two oil-recovery processes. The Peclet numbers proposed in this study are based on the primary fractures.

During primary production, oil is produced by fluid expansion. The pressure drops rapidly in the fractures because of the high permeability, while, in contrast, the matrix remains at higher pressure. This creates a pressure difference between the fracture and the adjacent matrix block, and in turn, leads to the flow of oil from the matrix to the fracture.

We define the Peclet number for primary production as the ratio of the time taken for the matrix to deliver 1 m^3 fluid to the time taken for the adjacent fracture to transport 1 m^3 fluid:

$$Pe \equiv \left(\frac{L^2/\alpha}{L^2 h\phi S_{oi} C_t \Delta p}\right) / [\mu_o L/(k_f dh\Delta p)] \tag{3}$$

where

$$\alpha = \frac{k_m}{\phi\mu c_t} \tag{4}$$

is the hydraulic diffusivity, h is the thickness of the model, C_t is the total compressibility, S_{oi} is the original oil saturation, Δp is the pressure difference, μ_o is the oil viscosity, k_f is the fracture permeability, L is the matrix (fracture) length and d is the fracture aperture. When *Pe* is large, the surrounding fractures are highly conductive compared to the matrix, while a small *Pe* indicates that the fractures are not efficient.

In waterflood, for the purpose of defining the Peclet number, we focus on counter-current imbibition. In this idealization, the injected water rapidly flows through the fracture network and surrounds a matrix block. If the matrix block is water-wet, the injected water imbibes into the matrix block because of capillary pressure.

The *Pe* for counter-current imbibition is defined as follows:

$$Pe \equiv \left[\frac{L^2/\alpha}{L^2 h\phi (S_{oi} - S_{or})}\right] / \left(\frac{1}{Qf_{wi}}\right) \tag{5}$$

where the capillary diffusion coefficient α is defined as:

$$\alpha(S_w) \equiv -\frac{k_m}{\phi} f_w \lambda_o \frac{dP_c}{dS_w} \tag{6}$$

with the water fractional flow f_w given by

$$f_w = \frac{k_{rw}/\mu_w}{k_{rw}/\mu_w + k_{ro}/\mu_o} \tag{7}$$

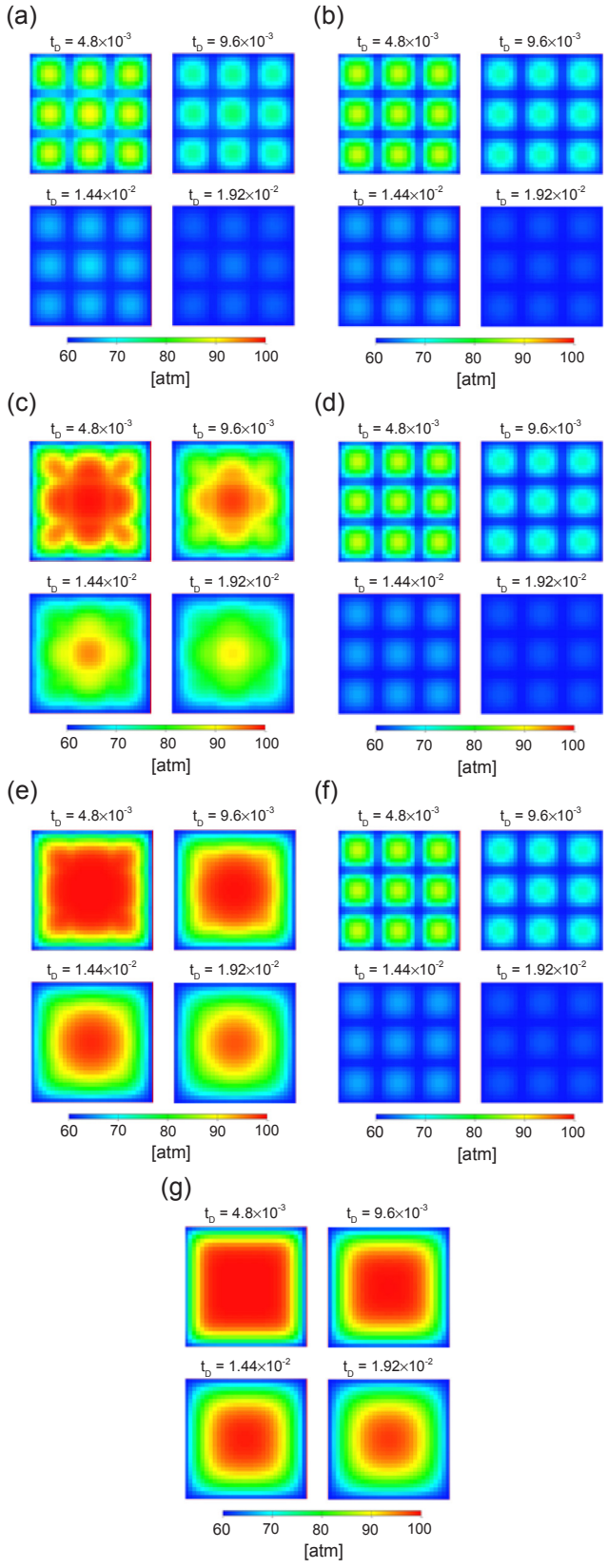

Fig. 5. Pressure distribution during primary production for different R_d with Pe = 10,000 and R_n = 1/3. (a) R_d = 5.8, with all fractures; (b) R_d = 5.8, with all average fractures; (c) R_d = 43.1, with all fractures; (d) R_d = 43.1, with all average fractures; (e) R_d = 79.4, with all fractures; (f) R_d = 79.4, with all average fractures; (g) without secondary fractures.

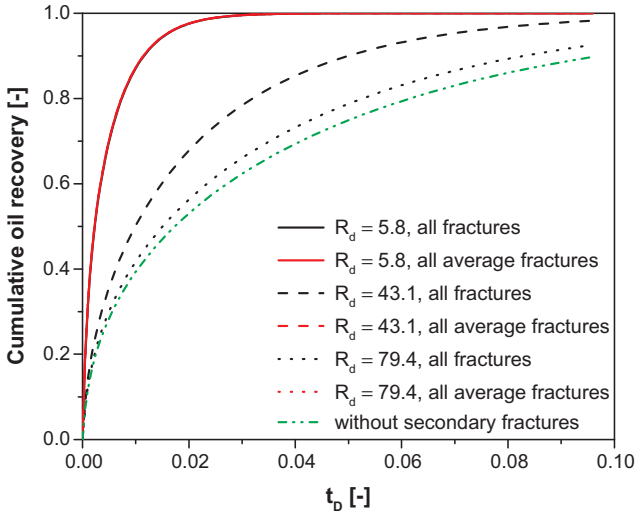

Fig. 6. Cumulative oil recovery during primary production for different R_d with Pe = 10,000 and R_n = 1/3. The curves for models with all average fractures for all three values of R_d overlie each other. The cumulative oil recovery is normalized by the producible oil for the given pressure reduction.

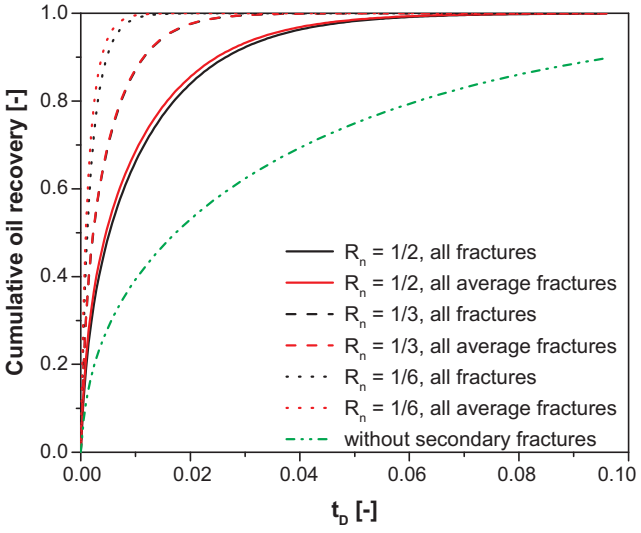

Fig. 7. Cumulative oil recovery during primary production for different R_n with Pe = 10,000 and R_d = 2.5.

where P_c is the capillary pressure, k_{rw} is the water relative permeability and k_{ro} is the oil relative permeability (all three are functions of S_w), and μ_w and μ_o are the water and oil viscosity, respectively. S_{oi} is the initial oil saturation, Q is the volumetric flow rate through the fracture and f_{wf} is the water fraction entering the fracture. The coefficient α is not a constant, but if one chooses an approximate average value for the recovery process, one can define a characteristic time. In this study, we apply a value of $\alpha = 1.9 \times 10^{-9}$ m^2/s, as discussed in the Appendix.

In addition, we consider two additional dimensionless groups:

- The ratio of the aperture d of the primary and secondary fractures (R_d). We specify an aperture of 1 mm for the primary fractures and vary the aperture of the secondary fractures in the cases with $R_d \leq 12.6$. In order to avoid possible numerical problems with extremely narrow fractures, in the cases with $R_d \geq 12.6$, we specify an aperture of 1 mm for all the fractures and make up the difference by adjusting the fracture permeability k_f. In these cases the fracture aperture we use in the ratio R_d is that corresponding to the same fracture transmissivity as in the simulation, i.e. (in m)

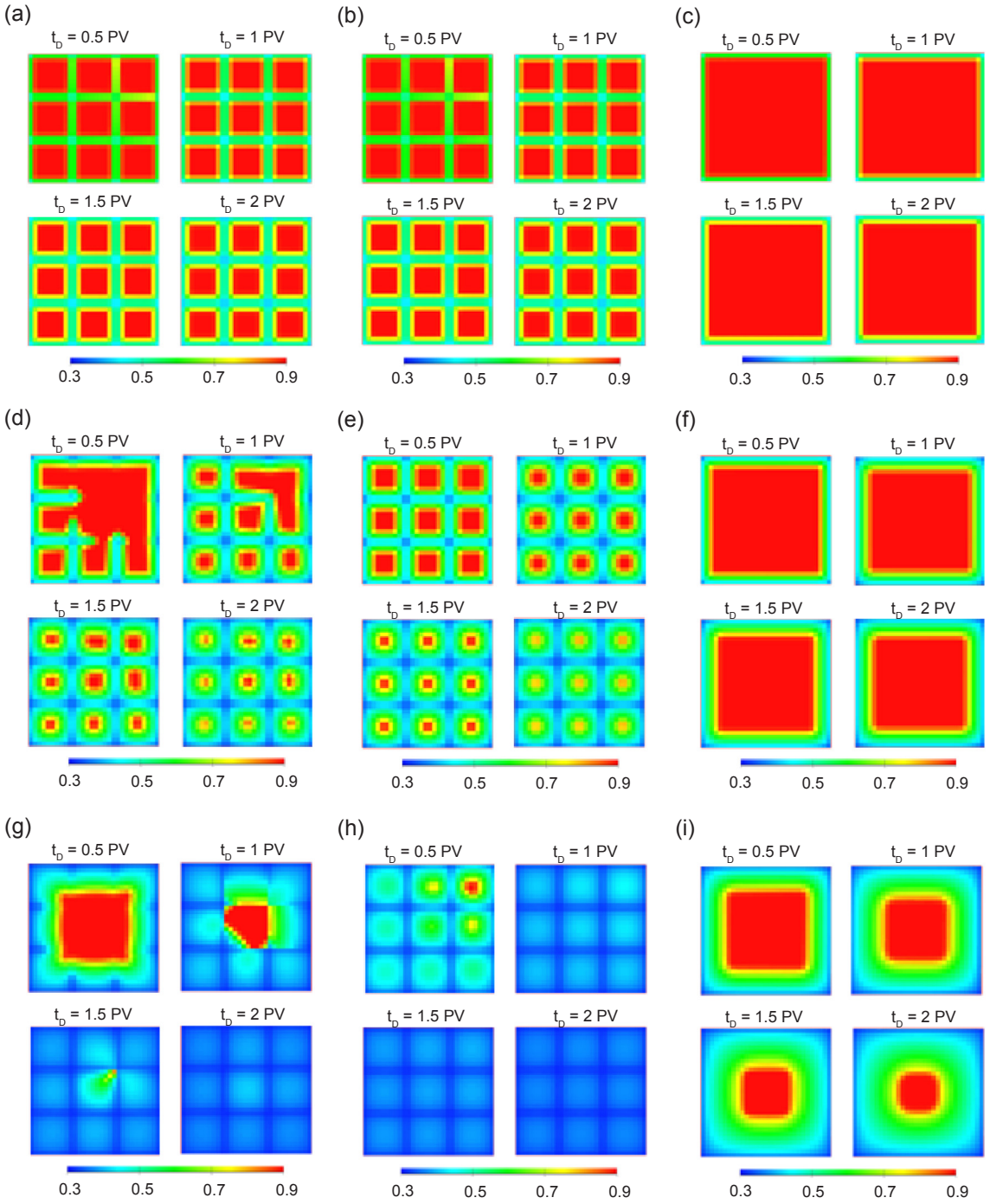

Fig. 8. Oil saturation during secondary production for different *Pe*, with $R_d = 2.5$, and $R_n = 1/3$. (a) *Pe* = 6,000, with all fractures, (b) *Pe* = 6,000, with all average fractures, (c) *Pe* = 6,000, without secondary fractures, (d) *Pe* = 600, with all fractures, (e) *Pe* = 600, with all average fractures, (f) *Pe* = 600, without secondary fractures, (g) *Pe* = 60, with all fractures, (h) *Pe* = 60, with all average fractures, (i) *Pe* = 60, without secondary fractures.

$[12 \times 10^{-3} k_f]^{1/3}$. Since the fracture permeability is defined as $d^2/12$, the ratio of permeabilities is square of the corresponding ratio of aperture. For example, for $R_d = 10$, the ratio of permeability of the primary and secondary fractures is 100. If the tertiary fractures are included, R_{d3} is the ratio between the apertures of primary and tertiary fractures.

- The ratio of the number of the primary fractures to the total number of the primary and secondary fractures (R_n) in a unit cell. Within a reservoir simulation, a unit cell is surrounded by other unit cells. Each fracture must accommodate flow from matrix blocks on both sides; therefore each primary fracture on the side of the matrix is considered as a half-fracture. Then, the total flow capacity of two (half-) primary fractures on opposite sides of the matrix is equal to that of one primary fracture. $R_n = 1/3$ approximately corresponds to our previous DFN study [15]. For a more complex reservoir, it might be better to correlate results to the cumulative lengths of primary and secondary fractures, as we did in our previous studies [15,16], rather than number of fractures. In this simplified representation, the fractures all have the same length, and R_n is also the ratio of cumulative fracture lengths.

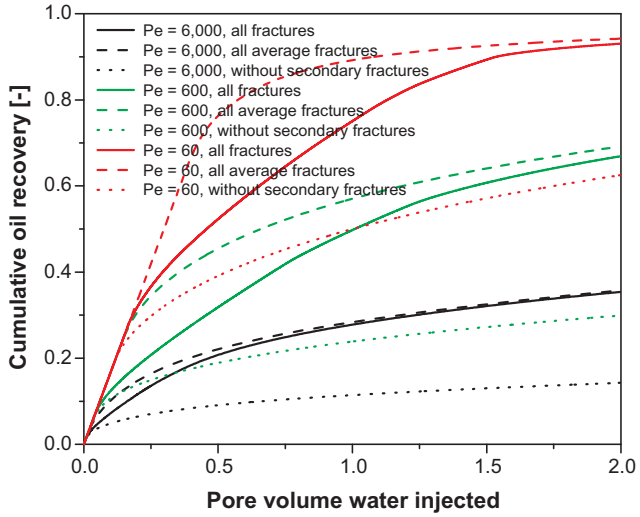

Fig. 9. Cumulative oil recovery during secondary production for different *Pe*, with $R_d = 2.5$ and $R_n = 1/3$. The cumulative oil recovery is normalized by the producible oil.

4. Results

4.1. Primary recovery

Since the Peclet number reflects the relative capacity of the fractures and the matrix to transport oil, we first present the flow patterns in the region studied with different values of the Peclet number, including some extreme cases in which the fracture permeability is very limited. The cumulative oil production and the pressure-distribution map are the bases for comparison. The results are presented as functions of dimensionless time t_D, defined by Eq. (A.3) in the Appendix. We compare the flow behavior of the fractured region with the original fracture network, the network with all fractures having the same aperture, which provides the same total conductivity of the original fracture network, and the network with secondary fractures excluded. Cumulative oil recovery is normalized by producible oil for the given process.

Fig. 3 shows the results for $R_d = 2.5$ and $R_n = 1/3$. This value of R_d and R_n approximates the results of our DFN study [15], i.e. that just 1/3 of the fractures account for 90% of the permeability of the fracture network. The pressure drops equally near both the primary and secondary fractures for $Pe = 1{,}000$; all the fractures are conductive enough to transport the oil delivered by the surrounded matrix blocks. In other words, all the fractures contribute equally (Fig. 3a and b) and the matrix limits oil production. For $Pe = 10$, all the fractures contribute nearly equally, but the fracture network limits oil production. For $Pe = 0.1$, even the primary fractures are unable to accommodate the matrix productivity, and the secondary fractures hardly matter. Oil recovery slows as *Pe* decreases, because the fractures are less able to transport oil produced by the matrix blocks (Fig. 4). For $Pe = 1{,}000$, treating all the fractures equally is a better approximation of the original fracture network than excluding the secondary fractures. Conversely, for $Pe = 10$ or less, excluding the secondary fractures provides a better approximation than treating all the fractures equally, though the error in excluding the secondary fractures is not large. These suggest that in calculation of the shape factor for a dual-porosity/dual-permeability model, for $Pe = 1{,}000$, all the fractures should be considered. For $Pe = 10$ or less, it is better to exclude the secondary fractures from the calculation of the shape factor than to include them and, in effect, assume they play an equally important role in transport to and from the matrix.

Fig. 5 shows the effect of R_d with $Pe = 10{,}000$ and $R_n = 1/3$. For $R_d = 5.8$ or less, the secondary fractures play a similar role to the primary fractures; they carry oil produced by the matrix blocks to the production well as efficiently as the primary fractures do. As R_d increases to 43.1, the flow capacity of the secondary fractures is much less than the primary fractures (but still 2,000 times more permeable than the matrix); the secondary fractures still deliver oil, but play a less-important role than the primary fractures. For $R_d = 79.4$, the secondary fractures only slightly affect oil recovery, and the flow pattern is very close to the case without the secondary fractures.

Fig. 6 compares the cumulative oil recovery of the original model, the model where all the fractures having the same aperture, and the model without the secondary fractures, for the values of R_d in Fig. 5. The curves for the models treating all the fractures equally important overlie each other for all the R_d values examined. For $R_d = 5.8$, the model where all the fractures having the same aperture provides a good approximation to the original model. As R_d increases (i.e., the secondary fractures become less permeable), the oil-production curve approaches that for the model without secondary fractures. For $R_d = 43.1$, oil production of the original model is approximately midway between that treating all the fractures equally important and that excluding the secondary fractures. In summary, if the secondary fractures are much narrower than the primary fractures, and *Pe* is large, the secondary fractures can be ignored without much loss of accuracy for simulation of primary production. Otherwise, treating the primary and secondary fractures equally approximates the original fractured region well during primary production.

Fig. 7 shows the effect of R_n (i.e., changing the number of the secondary fractures) with $Pe = 10{,}000$ and $R_d = 2.5$. The rate of oil recovery is heavily affected by R_n. But, again, the models that represent all the fractures as equally important provide a better approximation to the original models than those ignoring the secondary fractures.

4.2. Secondary recovery

The Peclet number for waterflood as defined in this study (Eq. (5)) depends on the injection rate and the water fraction in the injected fluid (f_{wI}). In most of the simulations below, $f_{wI} = 1$. The relative amounts of water carried by the primary and secondary fractures are dominated by the ratio of the aperture of the primary and secondary fractures (R_d) and the ratio of the numbers of the primary fractures to the total number of the primary and secondary fractures (R_n). In field application, $f_w = 1$ near an injection well, but further from an injection well it may be less if most injected water has already been imbibed into the matrix. Thus *Pe* would tend to be smaller at increasing distance from an injection well.

As noted above, the case with $R_d = 2.5$ and $R_n = 1/3$ approximates the flow distribution in our previous DFN study [15]. Fig. 8 shows the effect of *Pe* for this case. For $Pe = 6{,}000$, the injected water flowing through both the primary and secondary fractures is able to supply all the water that the matrix can imbibe (Fig. 8a). In this case, the fluid exchange between the matrix and both the primary and secondary fractures is counter-current imbibition. As the Peclet number decreases to 600, the injected water in the secondary fractures is unable to satisfy the adjacent matrix (Fig. 8d). The secondary fractures contribute to oil recovery by enabling co-current imbibition from the primary fractures, as confirmed by the examination of oil velocity at the face of the secondary fractures (not shown). Eventually, water reaches all the matrix blocks. For $Pe = 60$, the secondary fractures are less able to satisfy the adjacent matrix, but the matrix adjacent to the primary fractures expels oil by co-current imbibition. The role of co-current imbibition is evident in a comparison of Fig. 8 g and i: at $t_D = 0.5$ PV, oil is expelled more rapidly from the matrix adjacent to the primary fractures, if the secondary fractures are available to carry away the oil. The central matrix block, however, must wait for water from the secondary fractures. The secondary fractures provide a capillary barrier to co-current imbibition from the primary fractures.

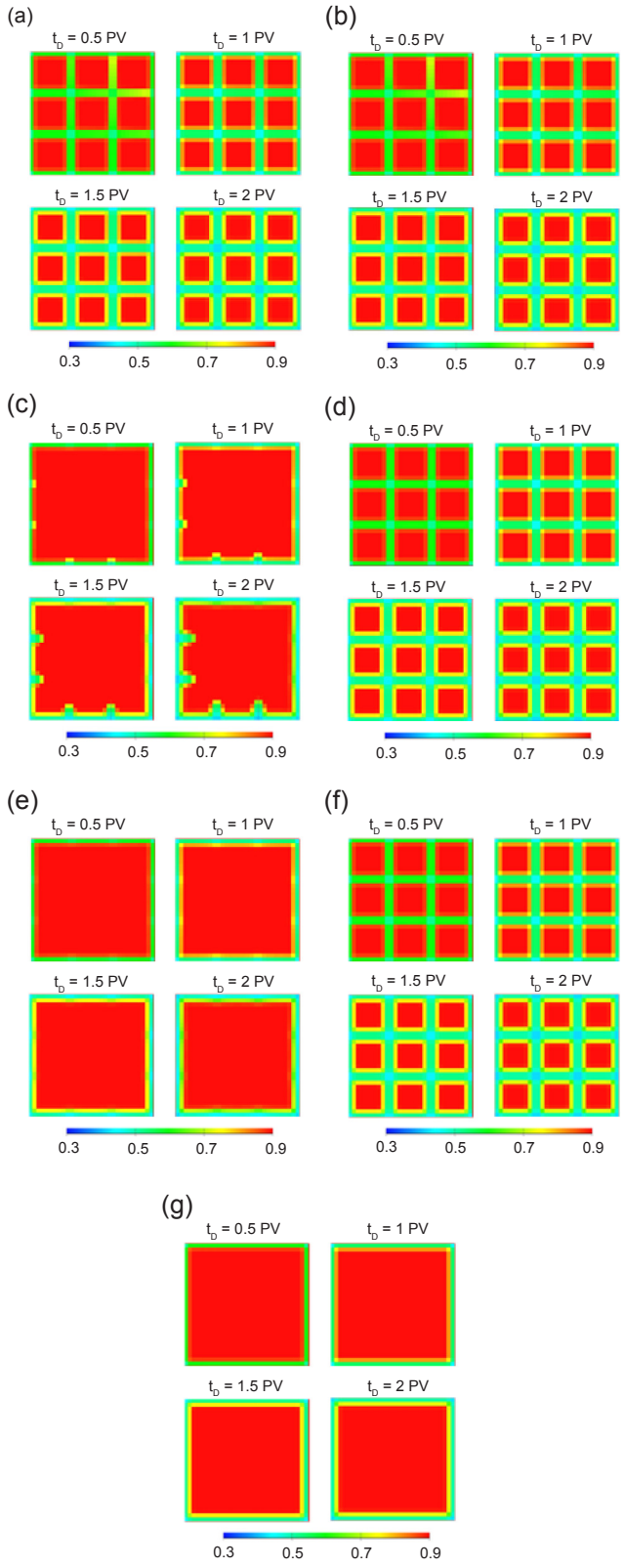

Fig. 10. Oil saturation during secondary production for different R_d, with Pe = 6,000, R_n = 1/3. (a) R_d = 2.5, with all fractures, (b) R_d = *2.5*, with all average fractures, (c) R_d = *6.3*, with all fractures, (d) R_d = *6.3*, with all average fractures, (e) R_d = *12.6*, with all fractures, (f) R_d = *12.6*, with all average fractures, (g) without secondary fractures.

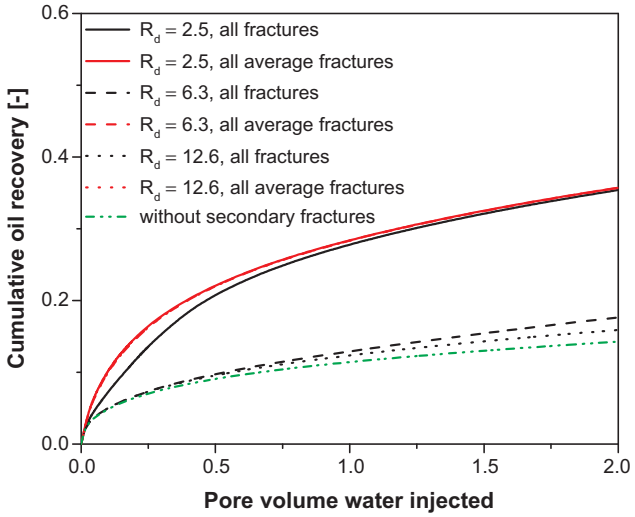

Fig. 11. Cumulative oil recovery during secondary production for different R_d, with Pe = 6,000 and R_n = 1/3. The cumulative oil recovery is normalized by the producible oil. All the cases with all average fractures overlie each other.

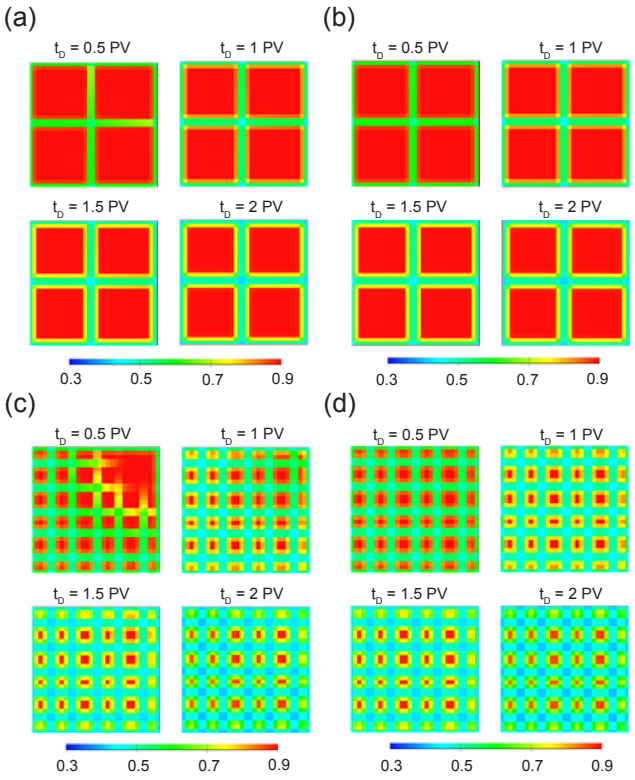

Fig. 12. Oil saturation during secondary production for different R_n, with Pe = 6,000 and R_d = 2.5. (a) R_n = 1/2, with all fractures, (b) R_n = 1/2, all average fractures, (c) R_n = 1/6, with all fractures, (d) R_n = 1/6, all average fractures.

Fig. 9 shows oil recovery for these cases. In all the cases, oil recovery is better approximated by treating all the fractures equally than by excluding the secondary fractures. For Pe = 600 or less, however, treating all the fractures equally overestimates oil recovery in the early stages. In none of the cases examined for the ratio of apertures (R_d = 2.5) based on our earlier DFN study [15] does simply excluding secondary fractures give a better approximation of oil recovery.

We next hold the Peclet number at Pe = 6,000 and vary the aperture ratio R_d. Fig. 10 shows that for R_d = 2.5, the injected water flows

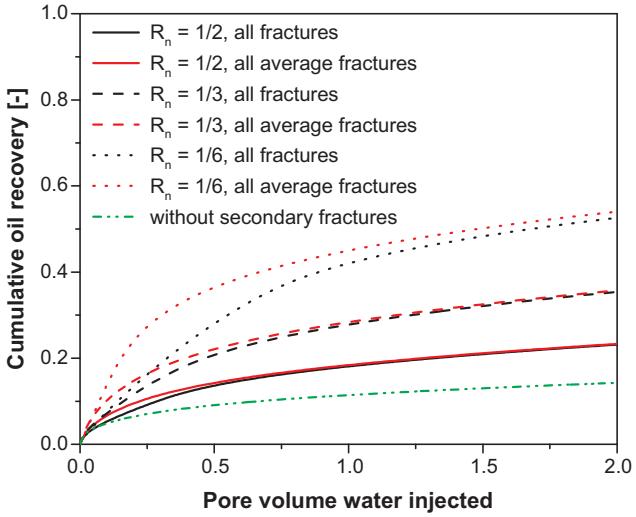

Fig. 13. Cumulative oil recovery during secondary production for different R_n, with Pe = 6,000 and R_d = 2.5. The cumulative oil recovery is normalized by the producible oil.

rapidly through both the primary and secondary fractures. Fluid exchange between the matrix and both the primary and secondary fractures is by counter-current imbibition. The primary fractures and secondary fractures play similar roles (Fig. 10a and b). Fig. 11 shows that the model treating all the fractures equally important gives a better approximation of the rate of oil recovery than the model without secondary fractures.

For R_d = 6.3, the injected water flow rapidly through the primary fractures, but slowly through the secondary fractures (Fig. 10c). For the matrix blocks bounded by both the primary and secondary fractures, the injected water imbibes into the matrix blocks from the primary fractures, and some oil flows into the secondary fractures, allowing co-current imbibition. Therefore, although the secondary fractures do not carry much injected water, they still provide paths for oil to flow to the production well. Nevertheless, Fig. 11 shows that for R_d = 6.3 or more, the model treating all the fractures equally important considerably overestimates oil recovery; the model excluding the secondary fractures provides a better approximation to the original model.

Figs. 12 and 13 show the effect of the ratio of the numbers of the primary fractures to the total number of the primary and secondary fractures (R_n) for Pe = 6,000 and R_d = 2.5. Treating all the fractures equally important approximates the flow behavior of the original model better than excluding the secondary fractures.

The very definition of the primary and secondary fractures, however, is affected by the truncation of the fracture distribution imposed by the length scale and the resolution of the fracture trace map. In reservoir simulations, considering the resolution of the fracture trace map of a field, as well as computational capacities, the set of fractures taken into account is truncated within a certain range. For a power-law distribution of apertures, very few of the narrowest fractures in the truncated distribution are among the primary fractures, and there would be many of these narrower fractures just below the aperture cut-off. For example, in our previous DFN study [15], the fractures are restricted to within a certain range of lengths (one order of magnitude) and apertures (three orders of magnitude). For broad aperture distributions, almost no primary fractures are near the lower limit of aperture. Thus if the distribution considered is extended to narrower fractures, there would be many narrower fractures in the distribution as a whole, but with little change in the primary fracture network. We therefore examine next the role that the excluded narrower fractures play during a waterflood process by including the tertiary fractures in the model. In this case, R_{d3} is the ratio of the apertures of the primary and tertiary fractures.

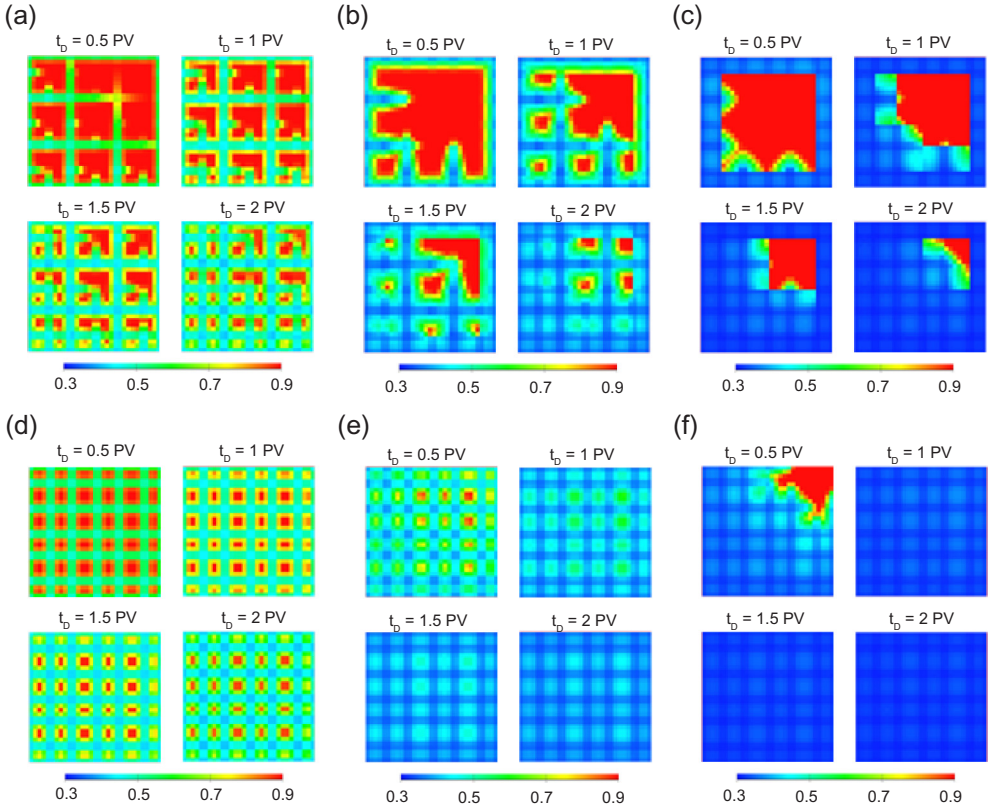

Fig. 14. Oil saturation during secondary production with tertiary fractures for different Pe. (a) Pe = 6,000, R_d = 2.5, R_{d3} = 5, (b) Pe = 600, R_d = 2.5, R_{d3} = 5, (c) Pe = 60, R_d = 2.5, R_{d3} = 5, (d) Pe = 6,000, with all average fractures, (e) Pe = 600, with all average fractures, (f) Pe = 60, with all average fractures.

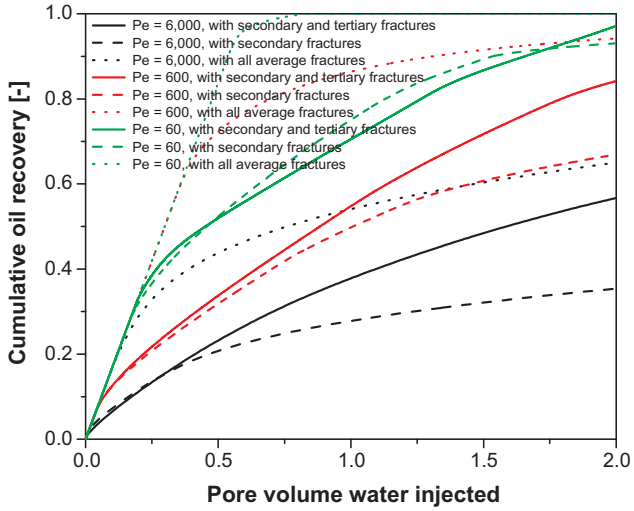

Fig. 15. Cumulative oil recovery during secondary production with tertiary fractures for different *Pe*, $R_d = 2.5$, $R_{d3} = 5$. The cumulative oil recovery is normalized by the producible oil.

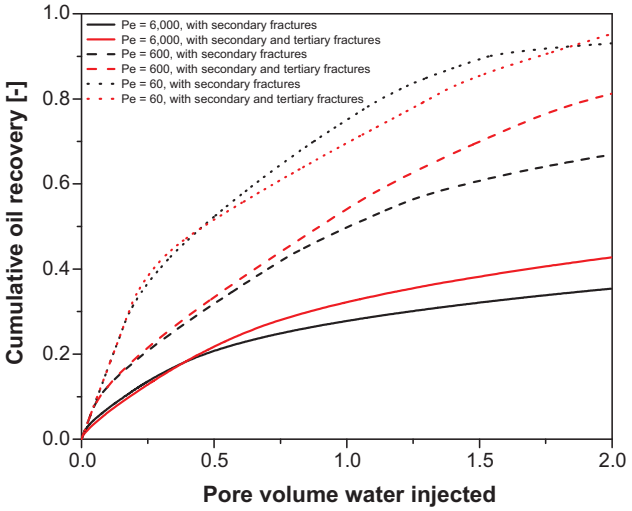

Fig. 17. Cumulative oil recovery during secondary production with tertiary fractures for different *Pe*, $R_d = 2.5$, $R_{d3} = 34.2$. The cumulative oil recovery is normalized by the producible oil.

In Figs. 14 and 15, the aperture ratio between the primary and secondary fractures is 2.5, and the tertiary fractures are half as wide as the secondary fractures ($R_{d3} = 5$). In all the cases, there are as many tertiary fractures as the primary and secondary fractures combined. The tertiary fractures play a role in producing oil, although they are not as important as the primary and secondary fractures. The tertiary fractures become less important as the Peclet number becomes smaller. When *Pe* decreases to 60, the tertiary fractures are not very helpful. Considering all the fractures to be equally conductive overestimates the oil recovery for all the values of *Pe* examined here. For $Pe = 60$, excluding the tertiary fractures leads to a more accurate prediction of oil recovery than treating them as equally important to the other fractures.

Figs. 16 and 17 show a more extreme case, with the aperture ratio between the primary and tertiary fractures (R_{d3}) set at 34.2. The injected water flows through the primary and secondary fractures and imbibes into the adjacent matrix, and then pushes oil into the tertiary fractures by co-current imbibition. The tertiary fractures help in producing oil in this case.

Figs. 18 and 19 show flow behavior of the fractured region with narrower secondary fractures ($R_d = 12.6$), and the tertiary fractures with the same aperture as in the previous case ($R_{d3} = 34.2$). For $Pe = 6{,}000$ and 600, the cases with and without tertiary fractures show similar oil recovery after 2 PV water is injected. When *Pe* decreases to 60, the oil residing in the matrix adjacent to the primary fractures is produced as in the case without the tertiary fractures, but the rest of the matrix, bounded by the tertiary fractures, hardly produces any oil. Evidently the tertiary fractures act as capillary barriers, not helping, but limiting, oil production.

In translating a fracture map to a DP/DK model, there are two issues: whether all the fractures contribute to recovery, and whether some may act as barriers to recovery.

The effect of the unavoidable truncation of a measured fracture distribution requires further study. The wider the range of fractures included, the larger the number of secondary (and yet-narrower) fractures included and the less accurate inclusion of all fractures on an equal basis in the definition of fracture spacing and shape factor. Excluding those fractures which are just above the truncation cut-off may have either no effect or a significant effect on the matrix-fracture exchange.

5. Conclusions

In this paper we consider the effect of heterogeneity in flow through a fracture network on the best characterization of the network for fractured reservoir simulations. The results depend on the relative flow rates through the primary and secondary fractures, represented here by

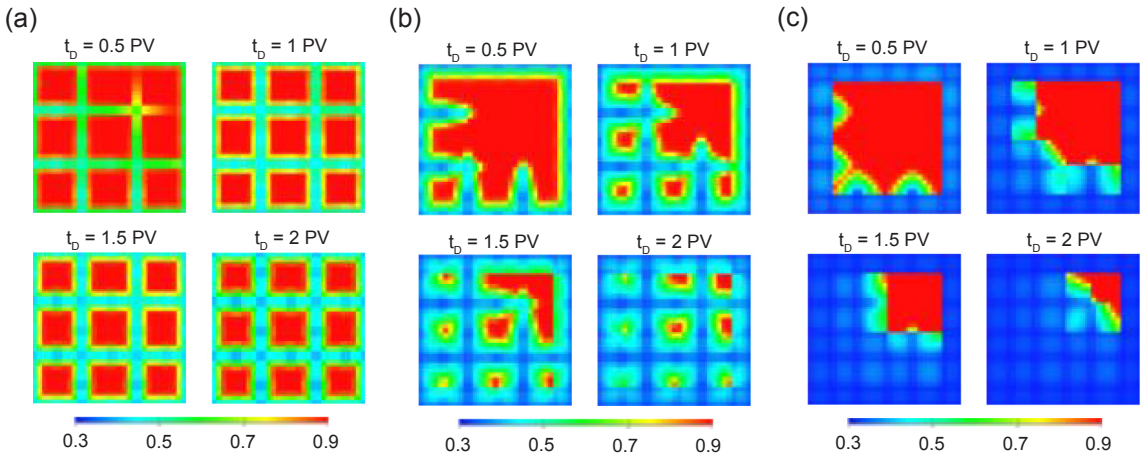

Fig. 16. Oil saturation during secondary production with tertiary fractures for different *Pe*. (a) $Pe = 6{,}000$, $R_d = 2.5$, $R_{d3} = 34.2$, (b) $Pe = 600$, $R_d = 2.5$, $R_{d3} = 34.2$, (c) $Pe = 60$, $R_d = 2.5$, $R_{d3} = 34.2$.

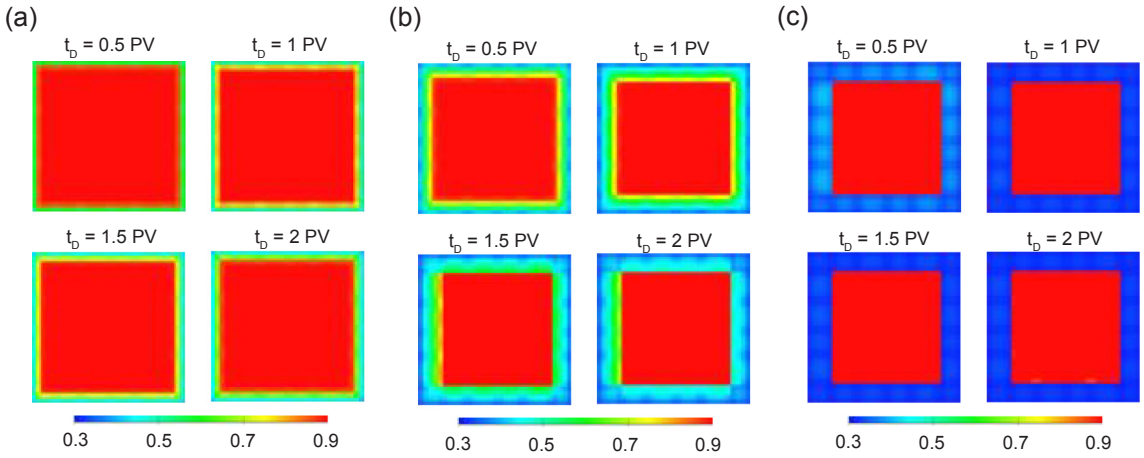

Fig. 18. Oil saturation during secondary production with tertiary fractures for different *Pe*. (a) Pe = 6,000, R_d = 12.6, R_{d3} = 34.2, (b) Pe = 600, R_d = 12.6, R_{d3} = 34.2, (c) Pe = 60, R_d = 12.6, R_{d3} = 34.2.

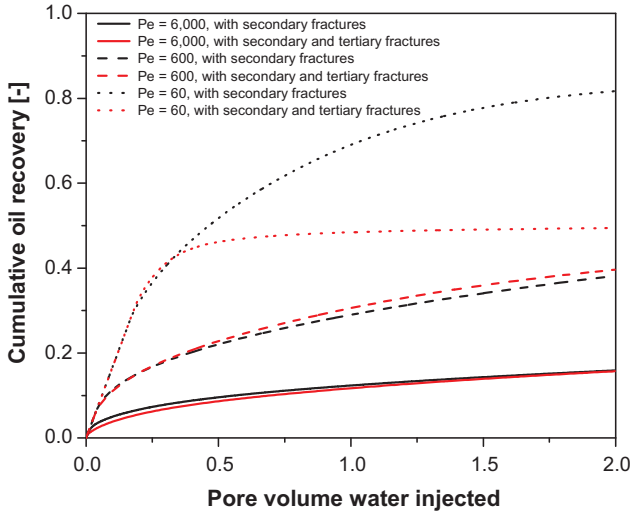

Fig. 19. Cumulative oil recovery during secondary production with tertiary fractures for different *Pe*, R_d = 12.6, R_{d3} = 34.2. The cumulative oil recovery is normalized by the producible oil.

the ratio of the aperture of the primary and secondary fractures, the ratio of the numbers of the primary fractures to the total number of the primary and secondary fractures, and the Peclet number defined in the Appendix. This Peclet number depends on the matrix and fracture properties for primary production and, for waterflood, on the flow rate and water fraction in the fracture network.

In primary production, for large Peclet number (Pe = 1,000), the secondary fractures are as important as the primary fractures. In other words, considering all the fractures to be equally conductive, as is assumed in a traditional DP/DK concept, provides a good approximation of matrix-fracture exchange. For a somewhat smaller Pe (10), the secondary fractures can help in producing oil, but play a less important role than the primary fractures. For a sufficiently small Peclet number (Pe = 0.1), the secondary fractures play a minor role; even the primary fractures are unable to accommodate the matrix productivity. Excluding the secondary fractures in that case gives a good approximation of the oil production, better than including them as equal to primary fractures. The best shape factor (characteristic fracture spacing) for DP/DK simulations should then only account for the primary fractures.

If R_d is small (< 5.8 in this study), the secondary fractures tend to play a similar role to the primary fractures. Both the primary and secondary fractures should be considered in the calculation of the characteristic fracture spacing or shape factor for a DP/DK simulation of a primary-production process. As R_d increases, the secondary fractures play a less-important role. As R_d increases to a large value (79.4 in this study), the secondary fractures can be excluded without affecting oil recovery. In other words, the secondary fractures should not be included in calculating the shape factor for DP/DK simulations of primary production in this scenario.

For large Peclet number (10,000) and R_d = 2.5, considering all the fractures as equally important provides a good approximation to the original model for all the value of R_n examined. The smaller the value of R_n is, the worse is the approximation given by excluding the secondary fractures.

For waterflood or EOR, in most cases examined, the appropriate shape factor should reflect both the primary and secondary fractures. In some cases (Pe = 600 and 60), the secondary fractures may not be as important as the primary fractures, but they still can play an important role by allowing co-current imbibition from the primary fractures and the adjacent matrix blocks.

If the secondary fractures are much narrower than the primary fractures (R_d = 6.3 or larger), however, they carry little injected water, and matter little to oil recovery. In those cases, excluding the secondary fractures provides a better approximation to the original model than considering all fractures equally. The characteristic fracture spacing or shape factor for a DP/DK simulation of a waterflood process in this situation should consider only the primary fractures.

For Pe = 6,000 and R_d = 2.5, in which the injected water can flow through all the factures efficiently, all the fractures are nearly equally important for all the values of R_n examined.

The fractures with an aperture below the cut-off of a truncated aperture distribution, referred to here as tertiary fractures, can be helpful in producing oil, although they are less important than the primary and secondary fractures. Tertiary fractures can also behave as capillary barriers and thereby limit oil recovery.

As shown in the Appendix, this definition of the Peclet number provided here works better than a previous published definition for the purpose of this study.

6. Discussion

During the last decades, much research has focused on topics related to the best shape factor for dual-porosity/dual-permeability simulations. There are at least three issues: (1) Can the diffusion process be approximated fundamentally with a first-order differential equation [20,31,32]? (2) How best to represent irregular-shaped matrix blocks as

simple shapes [18,19,27]? (3) How best to represent the matrix blocks with a distribution of sizes and odd shapes by a single shape factor [23,33,34]? In this study, we raise another issue: what fractures should be considered in calculation the characteristic fracture spacing or shape factor for dual-porosity/dual-permeability simulations? What factors does this depend on? Since this is an initial study, we start with simple models. There are many issues deserving further study:

Our focus in this study is limited to well-connected fracture networks; all the secondary (and tertiary) fractures are connected to the primary fractures. In nature, a fracture network may not be so well connected, which would change the flow behavior of the fractured region in some aspects. If the fracture aperture is related to fracture length, orientation, or stress, our results could be modified.

In addition, in this study, we have disregarded gravity-driven flow between the matrix and fractures, which could change the scaling of matrix-fracture exchange in secondary and tertiary recoveries.

In considering the effect of truncating a fracture network, one must consider that excluded fractures could either help or hinder oil recovery. The effect of truncation of the fracture distribution on our conclusions deserves further study.

In this initial study, the simplified geometry is highly symmetric. If there is no symmetry, as in real fracture networks, the matrix blocks shapes would be irregular, and vary in size. The rate that the fractures communicating with different blocks would be different. The effect of irregular shapes and diverse matrix block sizes on our conclusions needs further study.

Acknowledgments

We thank Saudi Aramco and the China Scholarship Council (CSC) for supporting our work. We thank Schlumberger for providing the academic license of ECLIPSE. We also thank Prof. Peter King for valuable discussions.

Appendix

Definition of Peclet number

A Peclet number indicates the relative importance of advection and diffusion to the transport of a physical quantity in a given system. In this study, it represents the relative capacity for oil transport of matrix production and fracture flow: i.e., how conductive fractures are compared to matrix productivity. We propose separate versions of the Peclet number for the two oil-recovery processes, primary and secondary recovery. The Peclet number proposed here is based on the spacing of primary fractures, without secondary fractures. We consider a square matrix block, of size $L \times L$, bounded by primary fractures, as illustrated in Fig. A.1. Within a reservoir, this region represents a unit cell surrounded by other unit cells. Each fracture must accommodate flow from matrix blocks on both sides; therefore the fracture permeability we assign, which accommodates flow from the given matrix block, is only half of the total fracture permeability. Then, because there are two (half-) fractures on opposite sides of the matrix in the two directions, the total flow capacity of the fractures surrounding the matrix block is equal to that of one fracture in each direction.

Definition of Pe for primary recovery

During primary production, oil is produced by fluid expansion from an initial pressure p to a reduced pressure (p-Δp). Pressure drops rapidly in the fractures, while the matrix initially remains at higher pressure. The pressure difference between the fracture and the adjacent matrix block drives oil from the matrix to the fracture. In comparing the flow capacities of the matrix and the fractures individually, we assume that each is unconstrained by the other. We assume a slightly compressible oil and incompressible water.

A one-dimensional (1D) primary-production process in matrix bounded by parallel fractures at uniform and constant pressure on opposite sides, is governed by [35–37]

$$\frac{\partial p}{\partial t} = \alpha \frac{\partial^2 p}{\partial x} \tag{A.1}$$

where

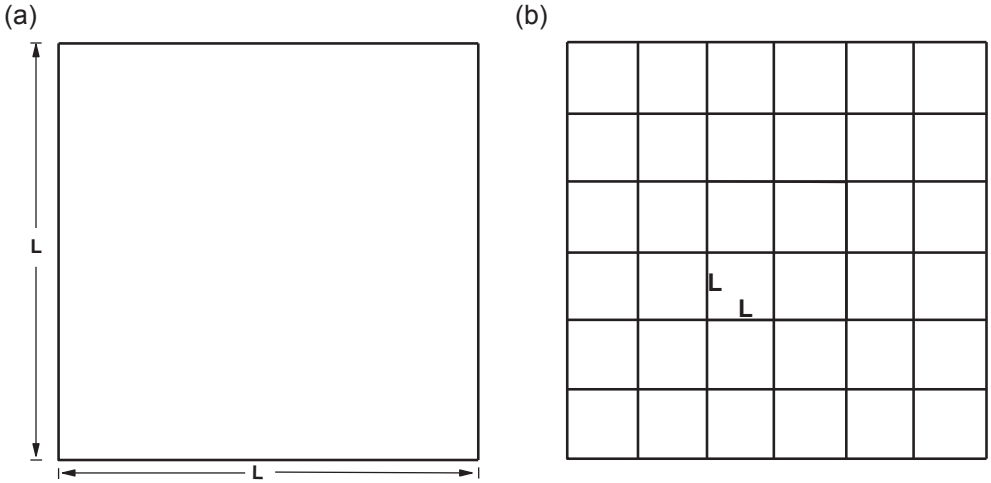

Fig. A.1. (a) Region of interest for defining Peclet number for matrix-fracture flow: a square matrix block bounded by the primary fractures, (b) schematic of a hypothetical simulation grid block containing 6 × 6 unit cells defined by the primary fractures.

$$\alpha = \frac{k_m}{\phi \mu_o c_t} \tag{A.2}$$

where p is the pressure, α is the hydraulic diffusivity, k_m is the matrix permeability, ϕ is the matrix porosity, μ_o is the oil viscosity, and c_t is the total fluid compressibility. We assume the oil is slightly compressible, so oil density is linearly related to pressure. Eq. (A.1) is in the form of the well-known equation governing unsteady heat conduction in a solid [35–37]. Recovery in a square matrix block is governed by the square of dimensionless average pressure derived from Eq. (A.1) [35]. The dimensionless time for this process is

$$t_D = \frac{\alpha t}{L^2} \tag{A.3}$$

We take the characteristic time t_c for the process as that at a dimensionless time of 1; thus

$$t_c = \frac{L^2}{\alpha} \tag{A.4}$$

Production is very uneven during this period, with production much faster at the start than at the end. Moreover, this characteristic time extends well beyond the period when almost all oil is recovered; we discuss this further below. Virtually all the oil is recovered by this time; the volume of oil recovered is $(L^2 h \phi S_{oi} C_t \Delta p)$, where S_{oi} is the initial oil saturation, ϕ is the matrix porosity, and h is the height of the system perpendicular to the cross-section shown in Fig. A.1. Averaged over the characteristic time, the time to produce one unit volume of oil is $\left(\frac{L^2/\alpha}{L^2 h \phi S_{oi} C_t \Delta p}\right)$.

For the fracture, we assume the same pressure difference Δp across the length of the fracture; this gives a flow rate of $\left(\frac{k_f d h \Delta p}{\mu_o L}\right)$, where k_f is the fracture permeability and d is the fracture aperture. The product $(k_f d)$ is the fracture transmissivity; for smooth slits, it equals $(d^3/12)$. The time for the fracture to transport one unit volume of oil is thus $\left(\frac{\mu_o L}{k_f d h \Delta p}\right)$. The Peclet number is the ratio of these two characteristic times:

$$Pe \equiv \left(\frac{L^2/\alpha}{L^2 h \phi S_{oi} C_t \Delta p}\right) / [\mu L/(k_f d h \Delta p)]. \tag{A.5}$$

If Pe is large, the surrounding fractures are relatively conductive compare to the matrix's ability to produce, while a small Pe indicates that the fractures are limiting on overall oil production.

Definition of Pe for secondary recovery by counter-current imbibition

In waterflood, for the purpose of defining Peclet number, we focus on counter-current imbibition. We assume counter-current imbibition is the dominant oil-recovery mechanism. This process governed by Eq. (A.1), with the coefficient α defined as

$$\alpha(S_w) \equiv -\frac{k_m}{\phi} f_w \frac{k_{ro}}{\mu_o} \frac{dP_c}{dS_w} \tag{A.6}$$

with water fractional flow f_w given by

$$f_w = \frac{k_{rw}/\mu_w}{k_{rw}/\mu_w + k_{ro}/\mu_o} \tag{A.7}$$

where P_c is the capillary pressure, k_{rw} is the water relative permeability and k_{ro} is the oil relative permeability (all three are functions of S_w), and μ_w and μ_o are the water and oil viscosities, respectively. Coefficient α is not a constant, but if one chooses an approximate average value for the recovery process [38], one can define a characteristic time using Eq. (A.1). Again, virtually all oil is recovered during this time; the volume recovered is $[L^2 h \phi (S_{oi} - S_{or})]$, where S_{or} is the residual oil saturation.

The fracture limits the process according to its ability to transport water to imbibe into the matrix and replace oil. The fracture supplies water at a rate $(Q f_{wI})$, where Q is the volumetric flow rate through the fracture and f_{wI} is the water fraction entering the fracture. As shown in Fig. A.2, the cumulative oil recovery is roughly the same for a constant volume of water injected into the fracture, for total flow rates varying by a factor of 20. The time for the fracture to provide one unit volume of water (which could displace one unit volume of oil from the matrix) is $[1/(Q f_{wI})]$. This leads to a Peclet number for counter-current imbibition defined by

$$Pe \equiv \left[\frac{L^2/\alpha}{L^2 h \phi (S_{oi} - S_{or})}\right] / \left(\frac{1}{Q f_{wI}}\right). \tag{A.8}$$

We assume a constant coefficient α for counter-current imbibition, only to define a Peclet number, not in our simulations of oil recovery. Nonetheless, a useful average value would apply approximately over the period of recovery of most of the oil. Fig. A.3 compares solutions for fraction of recoverable oil still in place (ROIP) in a 2D recovery process with various constant values of α to the numerical solution of the same process using the capillary-pressure and relative-permeability functions used in this paper (solid line). In the numerical solution, the fractures are flushed with large volumes of water so that fracture flow is not limiting on the rate of matrix recovery. A value of $\alpha = 1.9 \times 10^{-9}\,\mathrm{m}^2/\mathrm{s}$ gives a reasonable fit over the period in which 80% of the oil is recovered (Fig. A.3a). The fit is not so good at short times (Fig. A.3b). Nevertheless, this value suffices to roughly characterize the time scales of the recovery process.

Salimi and Bruining [14] proposed a definition of Peclet number for waterflood based on characteristic times without considering the volumes of oil residing in the matrix or fracture considered. The characteristic time for the fracture is then the time to replace the fluids in the fracture, whatever the fracture volume. This gives

$$Pe \equiv [L^2/\alpha] / \left(\frac{2Ldh}{Q f_{wI}}\right) \tag{A.9}$$

Fig. A.4 compares the Peclet number of Salimi and Bruining [14] to that defined by Eq. (A.8). In the reference case, $Pe = 6{,}000$, $R_d = 2.5$ and

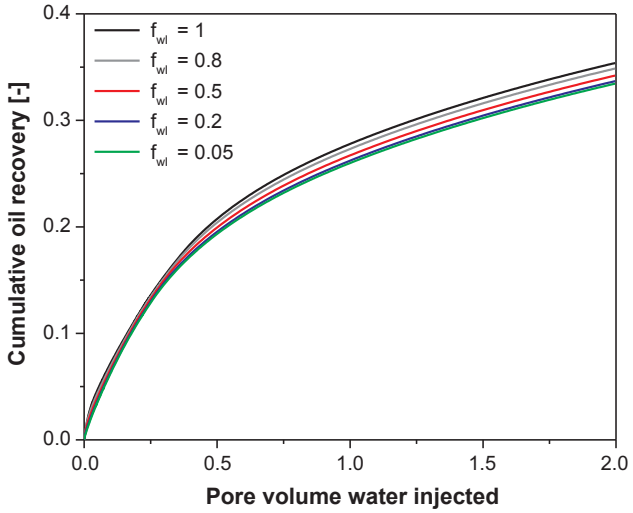

Fig. A.2. Cumulative oil recovery for different injected water fractions f_{wI} with a constant water injection rate Qf_{wI}, Pe = 6,000, R_d = 2.5, R_n = 1/3.

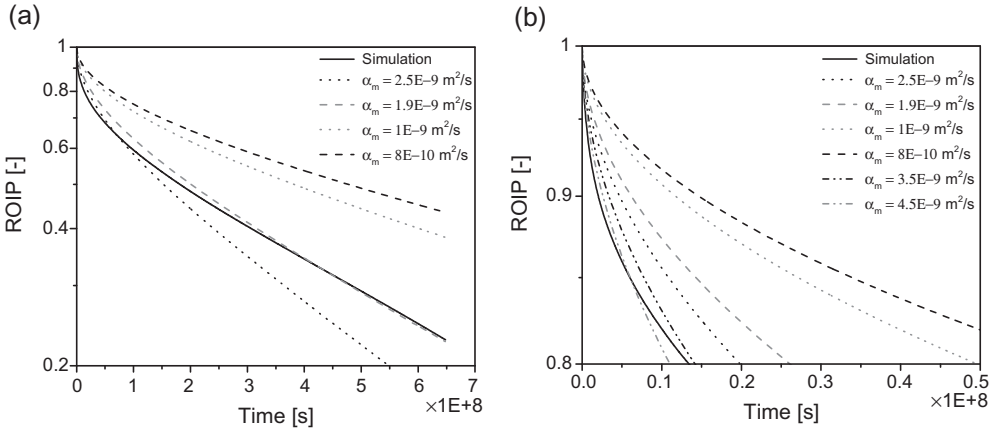

Fig. A.3. Fraction of remaining oil in place (ROIP) for a 2D recovery process calculated numerically (solid line) and with constant coefficient α for different values of α. (a) long time scale, during which most oil is recovered, (b) short times.

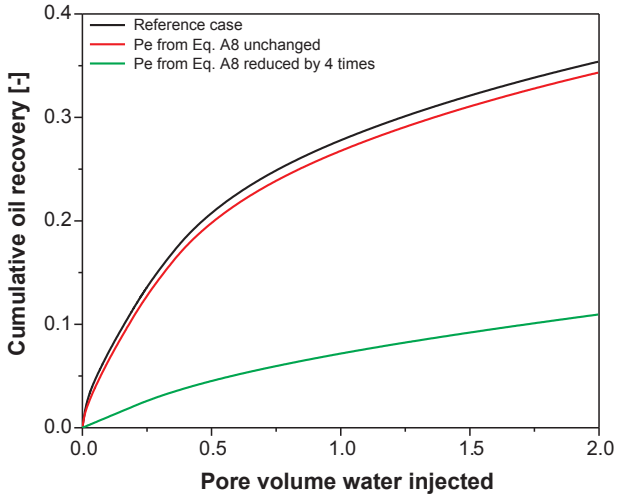

Fig. A.4. Comparison of oil recovery as a function of time for different definitions of Peclet number.

R_n = 1/3. In this case, the injected fluid flows rapidly through both the primary and secondary fractures. Primary and secondary fractures play similar roles. In the second case, the fracture length (L), thickness (h), porosity (ϕ) and permeability (k_m) of matrix blocks change to keep the value of Pe in Eq. (A.8) unchanged, while that of Salimi and Bruining doubles. In the third case, the value of Pe in Eq. (A.8) decreases four fold, while the value of Salimi and Bruining is unchanged. The capillary coefficient α remains the same. For the second case, the cumulative oil recovery is close to

the oil recovery of the reference case. In the third case, the cumulative oil recovery at a given time decreases by approximately a factor of 4, approximating the change in Eq. (A.8). Thus, the Peclet number defined in this study better fits the purpose of this study.

Interpreting the magnitude of Pe

As noted, even for a constant value of α, oil recovery is not constant in time for either primary or secondary recovery; the rate of oil recovery is much faster at the start than at the end. It is instructive to consider the time at which the flow capacities of the matrix and fractures are comparable, as a function of *Pe*.

We expect the fractures to be limiting only relatively early in the oil-recovery process, when production from matrix is greatest. For a constant α, for short dimensionless times t_D (less than 0.05), oil production in 1D scales with $\sqrt{t_D}$ [37]. The fraction of recoverable oil remaining in the square matrix region is approximately $(1-C_1\sqrt{\alpha t/L^2})^2$, with C_1 approximately 2.24 (obtained by a curve fit for the 1D recovery process in previous studies [36,37]). Therefore the rate of oil recovery from the matrix, if unlimited by the fracture flow capacity, is given by

$$Q_m = -\frac{d}{dt}[(L^2h\phi S_{oi}C_t\Delta p)(1-C_1\sqrt{\alpha t/L^2})^2] = (L^2h\phi S_{oi}C_t\Delta p)2(1-C_1\sqrt{\alpha t/L^2})C_1\frac{1}{2}\sqrt{\alpha/tL^2} \tag{A.10}$$

for primary production. The time at which this capacity equals the flow capacity of the matrix is likely to be short, for which the second term in brackets is approximately 1. Therefore

$$Q_m \approx (L^2h\phi S_{oi}C_t\Delta p)C_1\sqrt{\alpha/tL^2}. \tag{A.11}$$

The time at which the matrix flow capacity equals the fracture flow capacity is therefore given by

$$\left(\frac{k_f dh\Delta p}{\mu L}\right) \approx (L^2h\phi S_{oi}C_t\Delta p)C_1\sqrt{\alpha/tL^2}. \tag{A.12}$$

rearranging,

$$\sqrt{\alpha t/L^2} \approx (L^2h\phi S_{oi}C_t\Delta p)C_1(\alpha/L^2)\left(\frac{\mu L}{k_f dh\Delta p}\right) = C_1\left(\frac{1}{Pe}\right) \tag{A.13}$$

$$t_D \approx 5Pe^{-2} \tag{A.14}$$

where the dimensionless time t_D is defined in Eq. (A.3). For instance, for $Pe = 10$, the fractures would be limiting on oil recovery for $t_D \le 0.05$. The times in Fig. 3d-f are shorter than this, and the matrix-fracture exchange has progressed further in the matrix closer to the production well. For $Pe = 1{,}000$, the primary fractures are limiting for $t_D \le 5 \times 10^{-6}$, and in Fig. 3a-c the matrix-fracture exchange is nearly uniform along the primary fractures. For secondary recovery, a similar derivation leads to the same result, albeit assuming a constant value of α.

Interpretation of Pe for secondary fractures

We define *Pe* based on the network of primary fractures, and account for the secondary fractures using the dimensionless ratio of fracture apertures R_d and the number of primary fractures R_n. It is instructive to compare the values of *Pe* that would obtain from consideration of the matrix bounded by the secondary fractures. The size of the region is now $(L\ R_n) \times (L\ R_n)$. For both primary production and waterflood, the flow rate in the definition of Eqs. (A.5) and (A.9) is reduced by a factor of roughly R_d^{-3}. The value of *Pe* changes by a factor $\{(R_n^{-1})/[(R_d^{-3})]^{-1}\}$. For the case $R_n = 1/3$ and $R_d = 2.5$, the value of *Pe* for a matrix block surrounded by the secondary fractures is a factor $(3/2.5^3) \cong (1/5)$ of that based on the primary fractures. The fractures are somewhat less able to accommodate the flow capacity of the matrix. For larger values of R_d, the factor is smaller, e.g. 0.0015 for $R_d = 12.6$.

Interpretation of Pe for grid blocks in simulation

In a dual-porosity or dual-permeability simulation, a grid block represents a region containing many unit cells as defined above. Suppose there are $N_b \times N_b$ unit cells in the simulation grid block and consider fracture flow in one of the coordinate directions (*cf.* Fig. A.1b, where $N_b = 6$). There are N_b fractures to carry away oil or provide water, but N_b^2 matrix blocks to produce oil. The time to produce a unit volume of oil from the matrix grid block decreases by N_b^2 while the time for the fractures to provide a unit volume of water or carry away oil decreases by N_b; *Pe* decreases by a factor N_b. The pressure in the grid block and water fraction in the fractures is assumed uniform within a grid block in the dual-porosity/dual-permeability approach, but both vary from grid block to grid block and with time for any grid block. At each time, a new boundary condition is applied to matrix blocks by the changing conditions in the fractures. The state of the matrix is the superposition of the effects of all these changes. We propose that the value of *Pe* characterizing a grid block in a simulation corresponds roughly to that we propose for a unit cell, divided by the number of unit cells defined by the primary fractures across a simulation grid block.

In addition, *Pe* for secondary recovery depends on f_w in the fractures. Close to an injection well, $f_w \cong 1$. Further away, where the fractures carry both oil and water, both f_w and *Pe* would be reduced.

References

[1] Saidi AM. Reservoir engineering of fractured reservoirs (fundamental and practical aspects). Paris: Total Edition Press; 1987.

[2] Gilman JR, Kazemi H. Improved calculations for viscous and gravity displacement in matrix blocks in dual-porosity simulators. J Petrol Technol 1988;40:60–70.

[3] Hill AC, Thomas GW. A new approach for simulating complex fractured reservoirs. In: Middle east oil technical conference and exhibition, Society of Petroleum Engineers, Bahrain; 1985.

[4] Barenblatt GI, Zheltov IP, Kochina IN. Basic concepts in the theory of seepage of homogeneous liquids in fissured rocks [Strata]. J Appl Math Mech 1960;24:1286–303.

[5] Warren J, Root PJ. The behavior of naturally fractured reservoirs. SPE J 1963;3:245–55.

[6] Kazemi H, Merrill Jr LS, Porterfield KL, Zeman PR. Numerical simulation of water-

oil flow in naturally fractured reservoirs. SPE J 1976;16:317–26.
[7] Kim JG, Deo MD. Finite element, discrete-fracture model for multiphase flow in porous media. AlChE J 2000;46:1120–30.
[8] Karimi-Fard M, Firoozabadi A. Numerical simulation of water injection in fractured media using the discrete-fracture model and the Galerkin method. SPE Reserv Eval Eng 2003;6:117–26.
[9] Karimi-Fard M, Durlofsky LJ, Aziz K. An efficient discrete-fracture model applicable for general-purpose reservoir simulators. SPE J 2004;9:227–36.
[10] Geiger S, Roberts S, Matthäi SK, Zoppou C, Burri A. Combining finite element and finite volume methods for efficient multiphase flow simulations in highly heterogeneous and structurally complex geologic media. Geofluids 2004;4:284–99.
[11] Matthäi SK, Geiger S, Roberts S, Paluszny A, Belayneh M, Burri A, et al. Numerical simulation of multi-phase fluid flow in structurally complex reservoirs. Geol Soc, London, Spec Publ 2007;292:405–29.
[12] Li L, Lee SH. Efficient field-scale simulation of black oil in a naturally fractured reservoir through discrete fracture networks and homogenized media. SPE Reserv Eval Eng 2008;11:750–8.
[13] Dershowitz B, LaPointe P, Eiben T, Wei L. Integration of discrete feature network methods with conventional simulator approaches. SPE Reserv Eval Eng 2000;3:165–70.
[14] Salimi H, Bruining J. Improved prediction of oil recovery from waterflooded fractured reservoirs using homogenization. SPE Reserv Eval Eng 2010;13:44–55.
[15] Gong J, Rossen WR. Modeling flow in naturally fractured reservoirs: effect of fracture aperture distribution on dominant sub-network for flow. Pet Sci 2017;14:138–54.
[16] Gong J, Rossen WR. Shape factor for dual-permeability fractured reservoir simulation: effect of non-uniform flow in 2D fracture network. Fuel 2016;184:81–8.
[17] Cinco-Ley H, Samaniego V, Kucuk F. The pressure transient behavior for naturally fractured reservoirs with multiple block size. In: SPE annual technical conference and exhibition, Society of Petroleum Engineers, Las Vegas, Nevada; 1985.
[18] Heinemann Z, Mittermeir G. Derivation of the Kazemi–Gilman–Elsharkawy generalized dual porosity shape factor. Transp Porous Media 2012;91:123–32.
[19] Kazemi H, Gilman J, Eisharkawy A. Analytical and numerical solution of oil recovery from fractured reservoirs with empirical transfer functions. SPE Reserv Eng 1992;7:219–27.
[20] Landereau P, Noetinger B, Quintard M. Quasi-steady two-equation models for diffusive transport in fractured porous media: large-scale properties for densely fractured systems. Adv Water Res 2001;24:863–76.
[21] Mirzaei-Paiaman A, Masihi M. Scaling equations for oil/gas recovery from fractured porous media by counter-current spontaneous imbibition: from development to application. Energy Fuels 2013;27:4662–76.
[22] Noetinger B, Roubinet D, Russian A, Le Borgne T, Delay F, Dentz M, et al. Random walk methods for modeling hydrodynamic transport in porous and fractured media from pore to reservoir scale. Transp Porous Media 2016;115:345–85.
[23] Ranjbar E, Hassanzadeh H, Chen Z. One-dimensional matrix-fracture transfer in dual porosity systems with variable block size distribution. Transp Porous Media 2012;95:185–212.
[24] Rodriguez NR, Cinco-Ley H, Samaniego V. A variable block size model for the characterization of naturally fractured reservoirs. In: SPE annual technical conference and exhibition, Society of Petroleum Engineers, New Orleans, Louisiana; 2001.
[25] Ma S, Morrow NR, Zhang X. Generalized scaling of spontaneous imbibition data for strongly water-wet systems. J Petrol Sci Eng 1997;18:165–78.
[26] Zhang X, Morrow NR, Ma S. Experimental verification of a modified scaling group for spontaneous imbibition. SPE Reserv Eng 1996;11:280–5.
[27] Zimmerman RW, Bodvarsson GS. Effective block size for imbibition or absorption in dual-porosity media. Geophys Res Lett 1995;22:1461–4.
[28] Pooladi-Darvish M, Firoozabadi A. Cocurrent and countercurrent imbibition in a water-wet matrix block. SPE J 2000;5:3–11.
[29] Brooks RH, Corey AT. Hydraulic properties of porous media and their relation to drainage design. Trans ASAE 1964;7:26–8.
[30] Corey AT. The interrelation between gas and oil relative permeabilities. Producers Monthly 1954;19:38–41.
[31] Rangel-German ER, Kovscek AR. Time-dependent matrix-fracture shape factors for partially and completely immersed fractures. J Petrol Sci Eng 2006;54:149–63.
[32] Zimmerman RW, Chen G, Hadgu T, Bodvarsson GS. A numerical dual-porosity model with semianalytical treatment of fracture/matrix flow. Water Resour Res 1993;29:2127–37.
[33] Bourbiaux B, Granet S, Landereau P, Noetinger B, Sarda S, Sabathier J. Scaling up matrix-fracture transfers in dual-porosity models: theory and application. In: SPE annual technical conference; 1999.
[34] Jerbi C, Fourno A, Noetinger B, Delay F. A new estimation of equivalent matrix block sizes in fractured media with two-phase flow applications in dual porosity models. J Hydrol 2017;548:508–23.
[35] White FM. Heat and mass transfer. Addison-Wesley; 1988.
[36] Bird RB, Stewart WE, Lightfoot EN. Transport phenomena. Wiley; 2007.
[37] Akker HEA, Mudde RF. Transport phenomena: the art of balancing. Delft Academic Press; 2014.
[38] Rangel-German ER, Kovscek AR. Experimental and analytical study of multi-dimensional imbibition in fractured porous media. J Petrol Sci Eng 2002;36:45–60.